Study on Direct Dipolar Effect of Neighboring Protons in Proton Coupled ^{13}C Relaxation Experiment

Hyun Namgoong, Impyo Lee, and Jo Woong Lee*

Department of Chemistry and Institute of Molecular Science, College of Natural Sciences, Seoul National University, Seoul 151-742, Korea
Received June 19, 2000

The dipolar effect of neighboring protons that are not directly bonded to the carbon of interest on coupled carbon-13 relaxation in a simple organic molecule has been studied by comparing the relaxation behaviors of labeled carbon-13 in $Br^{13}CH_2COOH$ with those in $BrCH_2{}^{13}COOH$. Various pulse sequences, such as coupled inversion recovery pulse sequence, *J*-negative and *J*-positive pulse sequence, and nonselective and selective proton π pulse sequence, were employed to perform the required coupled spin relaxation experiments. To gain information on various spectral densities, including that of dipolar-CSA cross correlation, the experiments were performed on two different spectrometers, operating, respectively, at 50.31 and 125.51 MHz for ^{13}C. The magnitude of CH dipolar spectral densities for $BrCH_2{}^{13}COOH$ was found to be about 8% of those for $Br^{13}CH_2COOH$, which means the effect due to the protons not directly bonded to the carbon of interest is small but not completely negligible.

Introduction

In recent years the spin-lattice relaxation of scalar-coupled spin systems has been used to probe into molecular dynamics in solution.[1-6] Studying these relaxation processes enables the determination of a variety of ensemble averaged motional parameters that contain information on molecular structure and motions. Careful use of this technique, however, has required an isolated spin system, often necessitating extensive and laborious isotopic labeling of the molecule being studied. If this requirement could be relaxed, a much broader use of this method would be possible.

The contributions from protons not directly bonded to the carbon of interest have been deemed negligible when dealing with the relaxation of a $^{13}CH_2$ group in a hydrocarbon chain because these protons are located farther from the carbon than those directly bonded to it.[7] However, many investigators have disputed the validity of this simple approximation on the basis of their studies on the influence of neighboring spins, using molecules such as nonane,[7] ethanol[8] and adamantane.[9]

In the present study, we used two simple labeled bromoacetic acids $Br^{13}CH_2COOH$ and $BrCH_2{}^{13}COOH$ to explore the difference between the effect of protons directly and not directly bonded to the carbon-13 by comparing the relaxation of labeled carbon-13 in these two compounds. These two compounds each display a simple AX_2 type carbon spectrum and may be treated in a similar fashion. For carboxyl group carbon the chemical shift anisotropy (CSA) in general is known to play an important role, whereas for many methylene carbons it exerts only a very small influence and usually has been assumed negligible in the coupled relaxation model.[10] This approximation has proved satisfactory for interpreting the experimental data in most cases, especially when the data are taken at low magnetic fields (less than 4.7T). However, use of the higher fields, which have become widely available in recent years, requires greater care in the treatment of spin relaxation data since the chemical-shift anisotropy effects are proportional to the square of the magnetic field strength applied. But even at 500 MHz (*ca.* 11.75T), the CSA interaction is still weaker than the dipolar interactions and the relaxation induced by the CSA autocorrelation term will be small, and, as pointed out by Grant *et. al.*,[10] it can be included in the random-field relaxation terms because the CSA can be viewed as a pseudo first rank interaction.

However, the cross correlation between the dipolar and the CSA interactions, DD-CSA, which may be significant due to the larger dipolar interaction, introduces a relaxation pathway that may have some impact on the CH_2 coupled relaxation behavior. To confirm this idea we performed the experiments at both the lower and the higher magnetic field, *ca.* 4.7T and 11.74T, respectively. In the present study, the results obtained with and without consideration of DD-CSA cross-correlation are compared and used to gain information on the molecular dynamics of bromoacetic acid molecule in solution phase.

Theory

Since the quantum mechanical relaxation theory has been well presented elsewhere, we just provide here a brief outline of its essence in context with our present topic of interest.[11-16] The interaction Hamiltonian responsible for the relaxation of the spin system is in general expressed in terms of an irreducible spherical tensor basis as follows.

$$V(t) = \sum_k \sum_l \sum_{m=-l}^{l} (-1)^m U_{l,-m}(k,t) T_{l,m}(k), \qquad (1)$$

where the sum over *k* spans all the relevant relaxation mech-

*Corresponding author. E-mail: jwlee@nmrlab2.snu.ac.kr

anisms, with l and m the rank and projection indices, respectively, associated with the spherical tensors for the given mechanism, and with $U_{l,-m}(k,t)$ and $T_{l,m}(k)$ denoting the spatial and spin tensors in that order. We treat here the three important relaxation mechanisms for the CH_2 spin system: *intramolecular dipole-dipole interactions* (*DD*), *random field interactions* (*RF*), *cross-correlation between dipole-dipole and chemical shielding anisotropy interaction* (*CSA*). For these mechanisms the interaction Hamiltonian can be written as

$$V(t) = V(t)^{D\text{-}D} + V(t)^{RF} + V(t)^{CSA} \tag{2}$$

or

$$\begin{aligned} V(t) = &\sum_{i<j}\sum_{m=-2}^{2} (-1)^m U^{DD}_{2,-m}(ij,t)T^{DD}_{2,m}(ij) \\ &+ \sum_{i}\sum_{m=-1}^{1} (-1)^m U^{RF}_{1,-m}(i,t)T^{RF}_{1,m}(i) \\ &+ \sum_{m=-1}^{1} (-1)^m U^{CSA}_{2,-m}(ij,t)T^{CSA}_{2,m}(ij) \end{aligned} \tag{3}$$

The normalized irreducible spin operators for each term in Eq. (3) are expressed in standard angular momentum operator notations as

$$\begin{aligned} &T^{DD}_{2,0}(ij) = \sqrt{1/6}[4I^i_zI^j_z-(I^i_+I^j_- + I^i_-I^j_+)] \\ &T^{DD}_{2,\pm1}(ij) = \mp[I^i_zI^j_\pm + I^i_zI^j_\pm] \quad T^{DD}_{2,\pm2}(ij) = I^j_\pm I^j_\pm \\ &T^{RF}_{1,0}(i) = \sqrt{2}I^i_z \quad T^{RF}_{1,\pm1}(i) = \mp I^i_\pm \quad T^{CSA}_{2,0}(ij) = \sqrt{8/3}I_z \\ &T^{CSA}_{2,\pm1}(ij) = \mp I^j_\pm \quad T^{CSA}_{2,\pm2}(ij) = 0, \end{aligned} \tag{4}$$

and the corresponding lattice functions for the mth projection are given by

$$\begin{aligned} &T^{DD}_{2,m}(ij,t) = -\xi_{ij}Y_{2,m}(\theta_{ij}(t), \phi_{ij}(t)). \\ &U^{RF}_{1,m}(i,t) = \gamma_i\sum_k B_{1,m}(k,i,t) \\ &U^{CSA}_{2,m} = \delta/2[\sqrt{3/2}D^{(2)}_{0,m}(\Omega^{CSA}_i(t)) \\ &\qquad + \frac{\eta}{2}\{D^{(2)}_{2,m}(\Omega^{CSA}_i(t)) + D^{(2)}_{2,m}(\Omega^{CSA}_i(t))\}], \end{aligned} \tag{5}$$

where $Y_{2,m}$ and $B_{1,m}$, respectively, stand for the second-order spherical harmonics and the randomly modulated fields at the nucleus of interest, and D denotes the Wigner rotation matrix. Various constant terms have the following meanings:

$$\xi_{ij} = (6\pi/5)^{1/2}(\gamma_i\gamma_i\hbar r^{-3}_{ij}) \tag{6}$$

$$\delta = \sigma_{33}-\sigma_{iso}, \text{ and } \eta = (\sigma_{22}-\sigma_{11})/\delta, \tag{7}$$

where σ_{11}, σ_{22} and σ_{33} are the three principal values of the CSA tensor, and

$$\sigma_{iso} = (\sigma_{11} + \sigma_{22} + \sigma_{33})/3 \tag{8}$$

Spatial spectral power densities corresponding to various relaxation pathways are defined as follows.

$$J^{DD}_{ijkl}(\omega_{\alpha\beta}) = \xi_{ij}\xi_{kl}\int_0^\infty \langle Y_{2,0}(\Omega^L_{ij}(0))Y_{2,0}(\Omega^L_{kl}(t))\rangle \exp(i\omega_{\alpha\beta}t)dt \tag{9}$$

$$J^{RF}_{ij}(\omega_{\alpha\beta}) = \gamma_i\gamma_j\int_0^\infty \langle B_{1,0}(i,0)B_{1,0}(j,t)\rangle\exp(i\omega_{\alpha\beta}t)dt \tag{10}$$

$$J^{D\text{-}CDA}_{ijk}(\omega_{\alpha\beta}) = \xi^D_{ij}\xi^{CSA}_k\int_0^\infty \langle Y_{2,0}(\Omega^D_{ij}(0))Y_{2,0}(\Omega^{CSA}_k(t))\rangle \exp(i\omega_{\alpha\beta}t)dt \tag{11}$$

$$J^{CSA}_{k}(\omega_{\alpha\beta}) = \xi^{CSA}_k\xi^{CSA}_k\int_0^\infty \langle Y_{2,0}(\Omega^{CSA}_k(0))Y_{2,0}(\Omega^{CSA}_k(t))\rangle \exp(i\omega_{\alpha\beta}t)dt \tag{12}$$

To the second-order perturbation approximation the equation of motion for the reduced spin density matrix elements can be written in the following form of Redfield equation.[11]

$$\frac{dv_i(t)}{dt} = \sum_j R_{ij}[v_j(t) - v_j(\infty)] \text{ or } \frac{dv}{dt} = \boldsymbol{R}[v - v(\infty)], \tag{13}$$

where $\boldsymbol{R}$ represents the relaxation matrix in a given magnetization mode basis whose elements are defined as the expectation values of the zero projections of the irreducible spin product operators. Relaxation matrix elements in eigenstate basis may be written under the extreme narrowing condition as follows:

$$\begin{aligned} &R_{11} = -(20/3)J_{CH}-2j_C-4J^{CSA}_C, \quad R_{12} = -(5/3)\sqrt{2}J_{CH}, \\ &R_{13} = -2K_{HCH}, \quad R_{14} = -(7\sqrt{2}/3)K_{HCH}, \\ &R_{15} = -(4\sqrt{2})J^{D\text{-}CSA}_{CH,C}, \\ &R_{22} = -(10/3)J_{CH}-5J_{HH}-2j_C-4J^{CSA}_H, \\ &R_{23} = -2\sqrt{2}J_{CHH} \quad R_{24} = -(5/3)J_{HCH}+2K_{CH} \\ &R_{25} = -4J^{D\text{-}CSA}_{CH,H} \quad R_{26} = -4\sqrt{2}J^{D\text{-}CSA}_{HH,H} \\ &R_{27} = 4J^{D\text{-}CSA}_{HH,H} \\ &R_{33} = -4J_{CH}-2J_{HH}-2j_C-4j_H-4J^{CSA}_C-8J^{CS}_H \\ &R_{34} = \sqrt{2}(J_{HH} + J_{HCH} + 4K^{CSA}_{HH} + 2k_{HH}) \\ &R_{35} = -4\sqrt{2}(J^{D\text{-}CSA}_{CH,C} + J^{D\text{-}CSA}_{HH,H}) \\ &R_{36} = -8J^{D\text{-}CSA}_{CH,H} \quad R_{37} = 4\sqrt{2}K^{D\text{-}CSA}_{CH,H} \\ &R_{44} = -(14/3)J_{CH}-J_{HH}+(4/3)J_{HCH}-2j_C-4j_H+2k_{HH} \\ &\qquad -4J^{CSA}_C-(28/3)J^{CSA}_H+(16/3)K^{CS}_{HH} \\ &R_{45} = 4J^{D\text{-}CSA}_{HH,H} \quad R_{46} = 4\sqrt{2}K^{D\text{-}CSA}_{CH,H} \\ &R_{47} = -(28/3)J^{D\text{-}CSA}_{CH,H}+(16/3)K^{D\text{-}CSA}_{CH,H} \\ &R_{55} = -(16/3)J_{CH}-5J_{HH}-2K_{HCH}-2j_C-2j_H-4J^{CSA}_C-4J^{CS}_H \\ &R_{56} = \sqrt{2}(-(5/3)J_{CH}-2K_{CHH}) \quad R_{57} = (5/3)K_{HCH}+K_{CHH} \\ &R_{66} = -(20/3)J_{CH}-2J_{HH}-4j_H-8J^{CSA}_{HH} \\ &R_{67} = \sqrt{2}\{(10/3)K_{HCH}+J_{HH}4K^{CSA}_{HH}+2k_{HH}\} \\ &R_{77} = -(20/3)J_{CH}-J_{HH}+(10/3)K_{HCH}-4j_H+2k_{HH} \\ &\qquad -(16/3)J^{CSA}_H+(16/3)K^{CS}_{HH} \end{aligned} \tag{14}$$

All the symbols appearing in Eq. (14) are defined as originally described by Grant *et al.*[8] We can extract the information on the relaxation parameters by numerical curve fitting

of five different series of carbon-13 coupled relaxation data.

Experimentals and Calculations

NMR Sample Preparation and Experimental Conditions

Bromoacetic acids labeled at 1- and 2- ^{13}C positions, respectively, were purchased from Aldrich Chemical Co., Inc. and used without further purification. Both acetic acids were prepared as 1.00M solutions in $CDCl_3$ and sealed in 5mm NMR tubes after repeating the standard freeze-pump-thaw cycle five times to remove dissolved oxygen. The NMR experiments were performed on both Varian VXR-200S operating at the resonance frequency of 50.31 MHz for ^{13}C and Varian Unity-500 operating at the frequency of 125.51 MHz for ^{13}C. All observations were made over the spectral width of 400-600 Hz, focusing on the ^{13}C triplets of interest, with the acquisition time of 7-9 seconds. Typical π pulse width for inversion of the ^{13}C signal in the observing channel and for the ^{1}H signal in the decoupling channel were *ca.* 25 and 35 μs, respectively, on a Varian VXR-200S. The respective values were 22 and 18 μs on a Varian Unity 500. All measurements were performed at 298.15 ± 1 K.

Calculations of Parameters

General Considerations. Both the Downhill-Simplex fitting routine and Marquadt method[17] were used to minimize the sum of squares of the difference between the experimental and predicted magnetizations.

$$\chi^2 = \sum_{i=1}^{n}\sum_{j=1}^{m} [\nu_j^{\exp}(i) - \nu_j^{\mathrm{cal}}(i)]^2, \tag{15}$$

where the superscripts exp and cal refer to experimental and calculated values, respectively. Starting from a random initial set of parametric values, the iterating process is continued until minimum χ^2 is reached. The determined parameters are used to obtain theoretical evolution curves for various magnetizations, which are then compared with the experimentally derived ones.

Spectral Densities. Dipolar and random field spectral densities were obtained by fitting experimental data with Eq. (13). The boundary conditions required for $\nu(0)$, which means magnetization modes at $t = 0$, and $\nu(\infty)$, equilibrium magnetization modes at $t = \infty$, in various pulse sequence experiments may be expressed (including the correction factors necessary for compensation of experimental imperfections) as follows:

Coupled Inversion-Recovery Method (ci)

$$\nu_{ci}(0)=\begin{pmatrix} c_{\mathrm{ciC}} \\ G \\ d^i_{\mathrm{ci1}} \\ 0 \\ d^i_{\mathrm{ci2}} \\ 0 \\ 0 \end{pmatrix},\quad \nu_{\mathrm{ci}}(\infty)=\begin{pmatrix} 1 \\ G \\ d^e_{\mathrm{ci1}} \\ 0 \\ d^e_{\mathrm{ci2}} \\ 0 \\ 0 \end{pmatrix};\quad \nu_{\mathrm{ci}}(0)-\nu_{\mathrm{ci}}(\infty)=\begin{pmatrix} c_{\mathrm{ciC}}-1 \\ 0 \\ d_{\mathrm{ci1}} \\ 0 \\ d_{\mathrm{ci2}} \\ 0 \\ 0 \end{pmatrix} \tag{16a}$$

J-Negative Pulse Method (jn)

$$\nu_{\mathrm{jn}}(0)=\begin{pmatrix} d_{\mathrm{jn1}} \\ -Gc_{\mathrm{jnH}} \\ -c_{\mathrm{jnC}} + d^i_{\mathrm{jn3}} \\ 0 \\ d^i_{\mathrm{jn2}} \\ 0 \\ 0 \end{pmatrix},\quad \nu_{\mathrm{jn}}(\infty)=\begin{pmatrix} 1 \\ G \\ d^e_{\mathrm{jn3}} \\ 0 \\ d^e_{\mathrm{jn2}} \\ 0 \\ 0 \end{pmatrix};$$

$$\nu_{\mathrm{jn}}(0)-\nu_{\mathrm{jn}}(\infty)=\begin{pmatrix} d_{\mathrm{jn1}}-1 \\ G(1 + c_{\mathrm{jnH}}) \\ -c_{\mathrm{jnC}} \\ 0 \\ d_{\mathrm{jn2}} \\ 0 \\ 0 \end{pmatrix} \tag{16b}$$

J Positive Pulse Method (jp)

$$\nu_{\mathrm{jp}}(0)=\begin{pmatrix} d_{\mathrm{jp1}} \\ -Gc_{\mathrm{jpH}} \\ c_{\mathrm{jpC}} + d^i_{\mathrm{jp3}} \\ 0 \\ d^i_{\mathrm{jp2}} \\ 0 \\ 0 \end{pmatrix},\quad \nu_{\mathrm{jp}}(\infty)=\begin{pmatrix} 1 \\ G \\ d^e_{\mathrm{jp3}} \\ 0 \\ d^e_{\mathrm{jp2}} \\ 0 \\ 0 \end{pmatrix};$$

$$\nu_{\mathrm{jp}}(0)-\nu_{\mathrm{jp}}(\infty)=\begin{pmatrix} d_{\mathrm{jn1}}-1 \\ -G(1 + c_{\mathrm{jpH}}) \\ c_{\mathrm{jpC}} \\ 0 \\ d_{\mathrm{jp2}} \\ 0 \\ 0 \end{pmatrix} \tag{16c}$$

Nonselective Proton p π Pulse Method (pi)

$$\nu_{\mathrm{pi}}(0)=\begin{pmatrix} 1 \\ -Gc_{\mathrm{piH}} \\ d^i_{\mathrm{pi1}} \\ 0 \\ d^i_{\mathrm{pi2}} \\ 0 \\ 0 \end{pmatrix},\quad \nu_{\mathrm{pi}}(\infty)=\begin{pmatrix} 1 \\ G \\ d^e_{\mathrm{pi1}} \\ 0 \\ d^e_{\mathrm{pi2}} \\ 0 \\ 0 \end{pmatrix};$$

$$v_{pi}(0)-v_{pi}(\infty)=\begin{pmatrix}0\\-G(1+c_{piH})\\d_{pi1}\\0\\d_{pi2}\\0\\0\end{pmatrix} \quad (16d)$$

Selective Proton π Pulse Method (se)

$$v_{se}(0)=\begin{pmatrix}c_{seC}\\d_{se1}\\d^{i}_{se2}\\0\\Gc_{seH}+d^{i}_{se3}\\0\\0\end{pmatrix},\ v_{se}(\infty)=\begin{pmatrix}1\\G\\d^{e}_{se2}\\0\\d^{e}_{se3}\\0\\0\end{pmatrix};$$

$$v_{se}(0)-v_{se}(\infty)=\begin{pmatrix}-c_{seC}-1\\d_{se1}-G\\d_{se2}\\0\\Gc_{seH}\\0\\0\end{pmatrix}, \quad (16e)$$

where $G = \sqrt{2}(\gamma_H/\gamma_C)$

The correction factors appearing in the above expressions were introduced to compensate for the measurement errors stemming from various sources and, also, for effect due to the transverse relaxation occurring during the preparation period for the desired initial states.[2,18]

Results and Discussion

The spectral densities for the CH_2 spin system were obtained by non-linear least squares fitting of the experimental data using Eq. (13). Experimental errors arising from pulse imperfection, inhomogeneous magnetic field, delay time between the pulses and receiver system may bring about the discrepancies between the ideal relaxation curves and the experimental ones. Correction factors for each pulse sequence were introduced to compensate for these flaws, which are shown in Table 1 for the 1-carbon methylene moiety on Unity 500 spectrometer. As can be seen from Table 1, these values (c_i, d_i) are close to unity and zero, respectively. These correction factors of the various pulse sequences were found not to affect the observed spectral densities appreciably.

In Figure 1, three observable magnetization modes of 2-^{13}C of bromoacetic acid observed at the carbon resonance frequency of 125.51 MHz are shown. The relaxation curves of 2-carbon at the lower resonance frequency of 50.31 are similar to those shown in Figure 1. The NOE factors under the proton decoupling condition measured at these two different fields were also found to be similar in magnitude. We plotted the 1-carbon magnetization modes for each pulse perturbation in Figure 2. The coupled spectrum of 1-^{13}C shows a typical AX_2 triplet with a smaller coupling constant [J(C-H) = 4.63 Hz], but its restoration behaviors differ significantly from those of 2-carbon. First, as can be seen from Figures 2(b) and (c) there are no maxima in the relaxation curves of v_{+++} and v_{+-+} mode for the J-pulse sequences. This unusual situation can arise when there is a spectral density of the diagonal relaxation matrix element that is overwhelmingly large in magnitude compared with other spectral densities. Certainly the J_{HH} value obtained from the 1-carbon relaxation must be equal to that of the 2-carbon spin system. This quantity may weigh more heavily in 1-^{13}C relaxation than other dipolar spectral densities. The non-linear least square-fittings results presented in Tables 2 and 3 show that J_{HH} is greater than other spectral densities at least by an order of magnitude.

Table 1. A set of correction factors at 2-carbon moiety on 125.51 MHz

Pulse Seq.	*ci*	*jn*	*jp*	*Pi*	*Se*
c_C	0.94	0.83	0.84	–	0.93
c_H	–	1.05	1.12	1.06	0.89
d_1	-1.9×10^{-2}	6.0×10^{-3}	-8.0×10^{-2}	6.6×10^{-4}	-1.8×10^{-3}
d_2	-3.2×10^{-2}	4.6×10^{-3}	1.2×10^{-2}	8.6×10^{-3}	1.3×10^{-2}

In general, spectral densities have positive values causing the magnetizations to decay toward the equilibrium, but this is not always the case.[19] The sign of J_{HCH} can be determined from the coupled relaxation experiment. The v_{+-+} mode under normal carbon inversion recovery exhibits a positive or negative normalized intensity profile during the evolution depending on the sign of J_{HCH}.[20,21] This comes from the different recovery rate to equilibrium of the carbon central peak and outer lines.

In accordance with this, v_{+-+} modes under the proton 180°-pulse sequences are strongly influenced by J_{CHH}. Figures 2(d) and 2(e) show a decay pattern of magnetization v_{+-+} peculiarly different from those usually observed for other small organic molecules in the same ^{1}H-π pulse experiments. In view of the relaxation matrix in Eq. (14), it may be rationalized that the initial response of the magnetization mode v_{+-+} is determined mainly by the $R_{32} = 2\sqrt{2}J_{CHH}$ immediately after the proton inversion pulse. The sign of this cross-correlation spectral density can be easily predicted by simply looking at the restoration rate of two multiplet lines toward the equilibrium after the action of ^{1}H hard pulse. In the experiment reported here, 2-carbon v_{+-+} magnetization exhibits negative initial slope under the proton π pulse perturbation at both ^{13}C frequencies. This means that central carbon peaks restores more rapidly than those of the

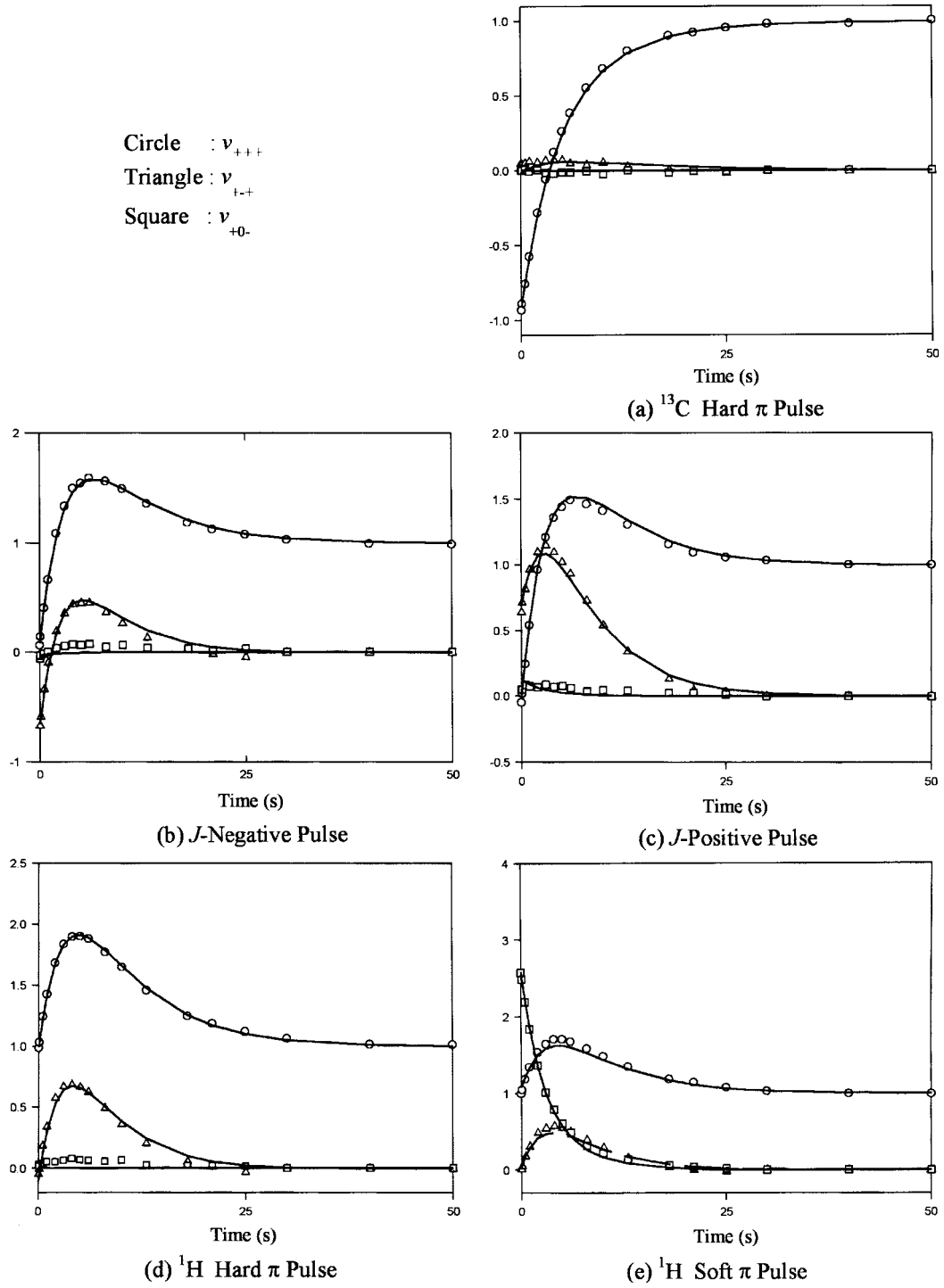

Figure 1. Plot of Magnetization of $Br^{13}CH_2COOH$ on Unity-500 at 298.15 K.

outer peaks. Fitted results also give us negative spectral density J_{CHH} at the remote 1-carbon system, which has never been reported previously. To see what condition gives rise to the negative carbon proton cross-correlation spectral density, we theoretically plotted J_{CHH}/J_{CH} as a function of motional anisotropy under the extreme narrowing condition as shown in Figure 3. The sign and magnitude of this ratio vary with the angle between the diffusion *z*-axis and the carbon-proton internuclear vector.[10] As this angle becomes larger than 130°, J_{CHH} changes its sign from positive to negative, assuming the chemical shift anisotropy remains invariant. Thus, even for the same molecule two different signs of J_{CHH} can be encountered depending on the molecular geometry. From this fact we could conclude that in this 1-carbon spin system the angle between the diffusion axis and carbon-proton internuclear vector seems to be larger than that of the normal methylene (CH_2) spin system (~90°) found in many organic samples.

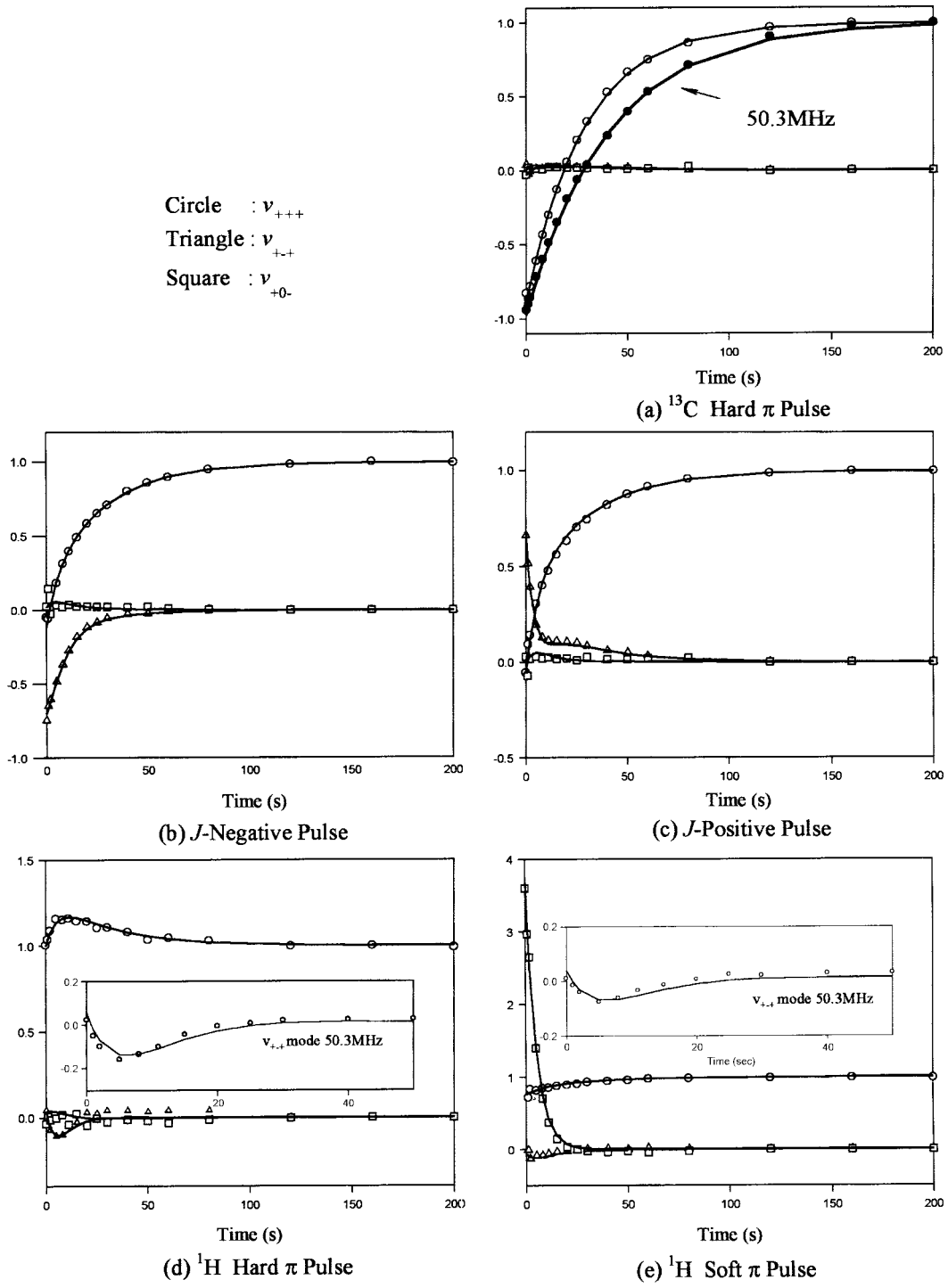

Figure 2. Plot of Magnetization of $BrCH_2{}^{13}COOH$ Including D-CSA Interaction on Unity-500 at 298.15 K.

Another noticeable experimental result is a relatively small NOE value for the 2-carbon of bromoacetic acid, which is not frequently observed in the usual CH_2 spin system. This reduction of NOE may be ascribed to the unusually large j_c originating mainly from scalar relaxation of the second kind.[13] (See Table 4). The irreducible spin operator related to the scalar relaxation of the second kind shows the same transformation property as the random field operator. Therefore it is impossible to know how much scalar relaxation of the second kind contributes to the total $j_{C.}$.[22] But we can at least understand that the presence of ^{37}Br resonating near the carbon-13 nuclei lowers the NOE value in 2-carbon in this manner.

Carbonyl carbon shows relaxation behaviors and NOE values quite different from those of methylene carbon, which is mainly due to the large chemical shielding anisotropy in the former. The total carbon magnetization mode decays more rapidly at higher field (125.51 MHz) than at

Table 2. Spectral densities of $Br^{13}CH_2COOH$ at 298.15 K

	$Br^{13}CH_2COOH$	
	VXR-200S	Unity-500
J_{CH}	2.46×10^{-2}	2.42×10^{-2}
J_{HH}	2.73×10^{-2}	2.77×10^{-2}
K_{HCH}	0.94×10^{-2}	0.88×10^{-2}
K_{CHH}	1.95×10^{-2}	2.01×10^{-2}
j_C	1.58×10^{-2}	2.24×10^{-2}
j_H	1.13×10^{-2}	1.35×10^{-2}
k_{HH}	1.09×10^{-2}	1.24×10^{-2}
χ^2	0.308	0.532

Table 3. Spectral densities of $BrCH_2{}^{13}COOH$ at 298.15 K

	VXR-200S	Unity-500	VXR-200S	Unity-500
J_{CH}	0.20×10^{-2}	0.22×10^{-2}	0.20×10^{-2}	0.22×10^{-2}
J_{HH}	2.73×10^{-2}	2.77×10^{-2}	2.73×10^{-2}	2.77×10^{-2}
K_{HCH}	0.07×10^{-2}	0.07×10^{-2}	0.07×10^{-2}	0.06×10^{-2}
K_{CHH}	-0.28×10^{-2}	-0.27×10^{-2}	-0.27×10^{-2}	-0.27×10^{-2}
J_C	0.63×10^{-2}	1.13×10^{-2}	0.55×10^{-2}	0.99×10^{-2}
j_H	1.13×10^{-2}	1.47×10^{-2}	1.13×10^{-2}	1.47×10^{-2}
k_{HH}	1.09×10^{-2}	1.25×10^{-2}	1.09×10^{-2}	1.16×10^{-2}
$J_{CH,C}^{D\text{-}CSA}$	0(locked)	0(locked)	1.02×10^{-4}	1.20×10^{-3}
$J_{CH,H}^{D\text{-}CSA}$	0(locked)	0(locked)	-0.10×10^{-4}	5.00×10^{-4}
$J_{HH,H}^{D\text{-}CSA}$	0(locked)	0(locked)	-0.55×10^{-4}	-1.25×10^{-3}
$J_{CH,H}^{D\text{-}CSA}$	0(locked)	0(locked)	0.95×10^{-4}	1.05×10^{-3}
χ^2	0.158	0.379	0.131	0.343

lower field (50.31 MHz) in normal carbon inversion recovery experiments, as shown in Figure 2(a). The NOE value at 125.51 MHz (~0.82) was found to be much smaller than that for normal protonated carbons. Therefore, for treatment of the relaxation of the 1-carbon spin system, we had to use the relaxation matrix that includes the CSA spectral density terms, and the results are presented in Table 4.

From the obtained values we confirmed that the long-range J_{CH} in 2-bromoacetic acid is much smaller than direct-bond J_{CH}. Considering the distance between the proton and carbon atom, long-range J_{CH} is expected to be only about one sixtieth of direct-bond J_{CH} in magnitude. But the ratio of long-range J_{CH} to direct-bond J_{CH} obtained from the separate coupled relaxation experiment was found to be larger than one-twentieth. Although this is still a small quantity, as pointed out by Fuson,[7] care must be exercised in utilizing the dipolar spectral density data for an AX_2 system surrounded by neighboring protons for elucidation of the molecular motion.

Unless the molecules have high symmetry about the nucleus of interest, the principal axes of the molecular diffusion tensor do not usually coincide with those of the chemical shift shielding tensor, which makes the situation more complicated. This problem was investigated by Goldman from the semi-group theoretical point of view.[23] If we

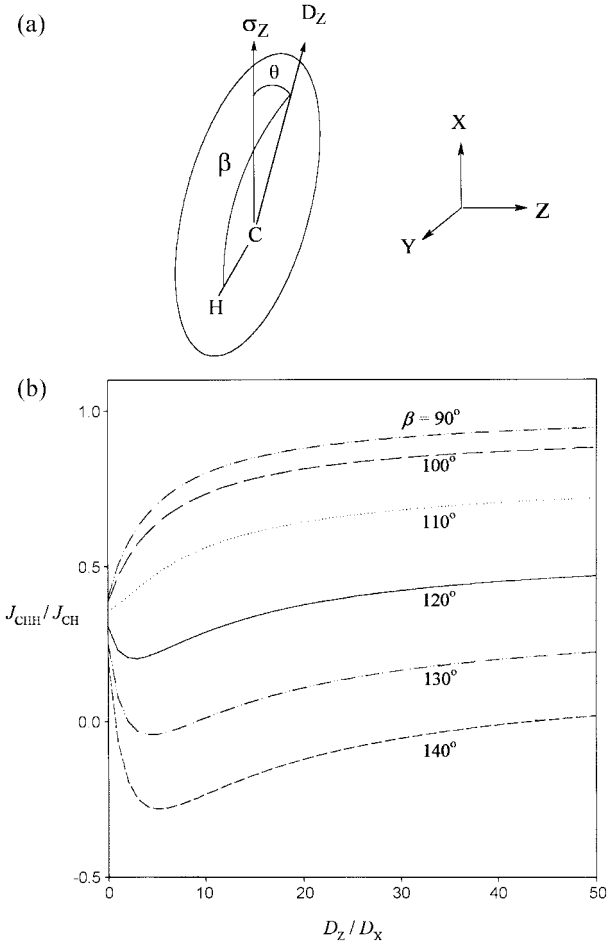

Figure 3. (a) Principal Axes of Diffusion Tensor and Chemical Shift Tensor for Arbitrary Oblate Symmetric Top Molecule (left), Laboratory Axis Frame (right). (b) Reduced Spectral Density (J_{CHH}/J_{CH}) as a Function of Anisotropy (D_Z/D_X) at Several β (Defined in Figure 3(a)).

assume that the CSA tensor has cylindrical symmetry and the *Z*-axis of the molecular diffusion frame is tilted away from the Z′-axis of the shift tensor, then Eq. (11) in isotropic phase can be rewritten through simple coordinate transformation in the following form:

$$J_{ijk}^{D\text{-}CSA}(\omega) = \xi_{ij}^{D}\xi_{k}^{CSA}\int_0^\infty \langle Y_{2,0}(\Omega_{ij}^{D}(0))Y_{2,0}(\Omega_{k}^{D}(0))\rangle \exp(i\omega t)dt\ P_2(\cos\theta), \quad (17)$$

where θ denotes the angle between the Z and Z' axis, and $P_2(\cos\theta)$ is the second order Legendre polynomial. This

Table 4. NOE factor calculated from obtained spectral densities at 298 K*[24]

	VXR-200S		Unity-500	
	$1\text{-}^{13}C$	$2\text{-}^{13}C$	$1\text{-}^{13}C$	$2\text{-}^{13}C$
Experimental data	1.13	1.56	0.82	1.53
Estimated by DD only	1.01	1.65	0.78	1.53
Estimated by including DD-CSA	1.02		0.84	

Table 5. Molecular parameters from the spectral densities

Frequency	50.31 MHz		125.51 MHz	
	2-carbon	1-carbon	2-carbon	1-carbon
D_X ($\times 10^{10}$)	1.09	1.08	1.09	1.12
D_Z ($\times 10^{10}$)	19.4	14.6	19.0	12.5
θ ($\angle ZZ'$)	51.1°		46.5°	
χ^2	0.334	1.41	0.673	1.39

result [Eq. (17)] implies that if the shielding anisotropy of carbon is known the magnitude in θ can be estimated. We performed an *ab initio* calculation using the Gaussian 94 HF/6-311+G(2d,p) // B3LYP/6-31G(d) for optimization and NMR calculation, which resulted in carbon shielding tensor principal values of 273.70, 136.71, and 110.09 ppm and the anisotropy of 100.2 ppm [δ in Eq. (7)]. Assuming that the present molecule has cylindrical symmetry both in chemical shift anisotropy and diffusion tensors, we estimated θ to be approximately 51.1° and 46.5° at 50.3 MHz and 125.51 MHz, respectively. (See Table 5). Since the principal axis frame of a molecule is, in general, not precisely known, these values of θ may not bear much quantitative sense. However, the approximate values of θ obtained in this manner give at least an indication that experimentally observed spectral densities may be used to resolve some equivocality in molecular structure determination.

In summary, the nonzero J_{CH} of $BrCH_2{}^{13}COOH$ indicates that the neighboring protons influence the carbon relaxation in a complicated manner. Therefore, neglecting the effect of neighboring protons, which has been ignored for simple geometrical reasons, can by no means be justified. In addition, new experimental features were revealed that negative dipolar spectral density J_{CHH} could result, depending on the molecular geometry, as observed in the 1-carbon CH_2 spin system in bromoacetic acid. Finally, to get more exact information on the molecular dynamics of the CH_2 spin system *via* coupled relaxation experiments, we recommend that protons in close spatial proximity to this spin system be deuterated.

Acknowledgment. This research was supported by the Korea Research Foundation (Grant No. 1998-015-D00148) of Ministry of Education.

References

1. Fuson, M. M.; Prestegard, J. H. *J. Am. Chem. Soc*. **1983**, *105*, 168.
2. Grant, D. M.; Mayne, C. L.; Liu, F.; Xiang, T.-X. *Chem. Rev.* **1991**, *91*, 1591.
3. Mayne, C. L.; Grant, D. M.; Alderman, D. W. *J. Chem. Phys.* **1976**, *65*, 1684.
4. Brow, M. S.; Grant, D. M.; Horton, W. J.; Mayne, C. L.; Evans, G. T. *J. Am Chem. Soc.* **1985**, *107*, 6698.
5. Fuson, M. M.; Grant, D. M. *Macromolecules* **1988**, *21*, 944.
6. Ahn, S.; Lee, J. W. *Bull. Korean Chem. Soc.* **1994**, *15*, 553.
7. Fuson, M. M.; Belu, A. M. *J. Magn. Reson. A* **1994**, *107*, 1.
8. Zheng, Z.; Mayne, C. L.; Grant, D. M. *J. Magn. Reson. A* **1993**, *103*, 268.
9. Brondeau, J.; Canet, D.; Millot, C.; Nery, H.; Werbelow, L. *J. Chem. Phys*. **1985**, *82*, 2212.
10. Werbelow, L. G.; Grant, D. M. *Adv. Magn. Reson.* **1979**, *9*, 189.
11. Redfield, A. G. *Adv. Magn. Reson.* **1965**, *1*, 1.
12. Hubbard, P. S. *Rev. Mod. Phys.* **1961**, *33*, 249.
13. Abragam, A. *The Principles of Nuclear Magnetism*; Oxford University Press: Oxford, U. K., 1961; p 309.
14. Canet, D. *Prog. NMR Spectrosc.* **1989**, *21*, 237.
15. Vold, R. L.; Vold, R. R. *Prog. NMR Spectrosc.* **1978**, *12*, 79.
16. McConnel, J. *The Theory of Nuclear Magnetic Relaxation in Liquid*; Cambridge University Press: U. S. A., 1987.
17. Press, W. H.; Flannerey, B. P.; Teukolsky, S. A.; Vetterling, W. T. *Numerical Recipes in Fortran*; Cambridge University Press: U. S. A., 1989.
18. Lim, P. H. *Ph. D Thesis*; S. N. U., 1998.
19. Brown, M. S.; Mayne, C. L.; Grant, D. M.; Chou, T. C.; Allored, E. L. *J. Phys. Chem.* **1984**, *88*, 2708.
20. Namgoong, H. *Ph. D Thesis*; S. N. U., 2000.
21. Daragan, V. A.; Mayo, K. H. *Prog. NMR Spectrosc.* **1997**, *31*, 63.
22. Canet, D.; Robert, J. B. *NMR at very high field*; Springer, 1991.
23. Goldman, M. *J. Magn. Reson.* **1984**, *60*, 437.
24. The NOE factor reported by D.Canet in ref 14 has minor typographical errors. The correct one should read as follows

$$\eta_{C-\{H\}} = 2\frac{\gamma_H}{\gamma_C}\frac{\sigma_{CH}K_1(R_{13}+\sqrt{2}R_{14})K_2}{T_{1,C}^{-1}K_1+(R_{13}+\sqrt{2}R_{14})^2(R_{66}+2R_{77}+2\sqrt{2}R_{67})}$$

$$T_{1,C}^{-1} = -R_{11} \qquad \sigma_{CH} = -R_{12}/\sqrt{2}$$

$$K_1 = (R_{36}+2R_{47})^2 - (R_{33}+2R_{44}+2\sqrt{2}R_{34})(R_{66}+2R_{77}+2\sqrt{2}R_{67})$$

$$K_2 = (R_{36}+2R_{47})(R_{26}/\sqrt{2}+R_{27}) - (R_{66}+2R_{77}+2\sqrt{2}R_{67})(R_{23}/\sqrt{2}+R_{24})$$